

Characterizing Seismic Scattering in the P-Wave Coda Using Rotational Seismology

Jonah Bartrand¹ and Robert Abbott²

¹ University of Idaho, ² Sandia National Laboratories



Introduction

Only recently have portable rotational seismometers achieved the necessary sensitivity for field deployments. Using six degree-of-freedom seismic data collected from a prototype rotational seismometer and a posthole translational seismometer, we investigated the possibility of comparing rotational and translational seismogram magnitudes in the P-wave coda to locate subsurface scattering locations.

Theory

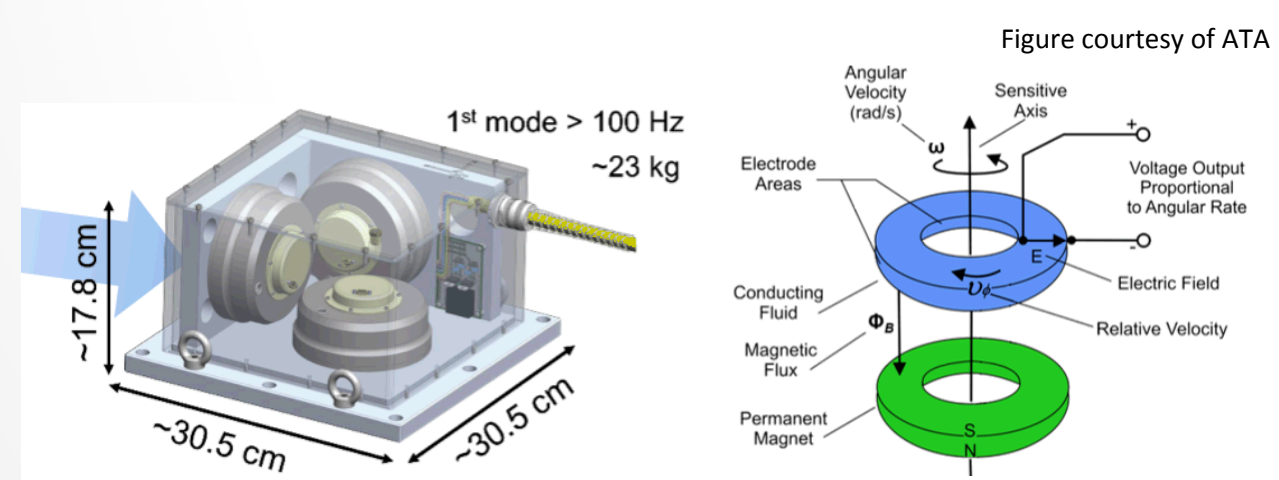
Rotational seismometers are not sensitive to compression waves (P-waves). Because compression waves travel faster than shear waves (S-waves), any rotational signal observed in the interval between the P-wave arrival and the S-wave arrival should be caused by P-wave conversions to S-waves between the source and the receiver. By determining the travel time difference from the observed rotational signal to the direct S-wave arrival (and knowing the S-wave velocity), one can estimate the scattering location.

Site Configuration

The data was gathered as part of a larger geophysical site characterization of the HADDOCK legacy underground nuclear test on the Nevada National Security Site. HADDOCK did not result in a visible surface crater. Using the Seismic Hammer (13,000 kg mass dropped from 1.5 meters) as a seismic source, 287 shots were taken on an array centered on the test, with shots taken as far as 1 km from the chimney. A 3-axis Trillium Compact Posthole translational seismometer and a 3-axis ATA Proto-SMHD Rotational seismometer were co-located near the test borehole (Figure 1.) The subsurface geology of the area has been extensively mapped (Figure 4), so fault locations are known.

ATA Sensor

We used a prototype 3-axis rotational seismometer developed by ATA. The sensor for each axis consists of a ring of electrically conductive fluid and a permanent magnet. When the sensor rotates, the magnet moves, relative to the fluid, inducing a voltage across the fluid which is proportional to rotation rate and is measured by electrodes.



Single-Point Scattering

To determine the scattering location, we assumed a single scattering event per sub-interval. The temporal distance from the center of each sub-interval to the S-wave arrival was mapped to a spatial location using the P- and S-wave speed profiles, which are generated from the manually-picked wave arrivals. The mathematical formulation is as follows:

$$\Delta t * \frac{v_p(d) * v_s(d)}{v_p(d) - v_s(d)} = d$$

Where Δt is the time to S-arrival and d is the scattering distance.

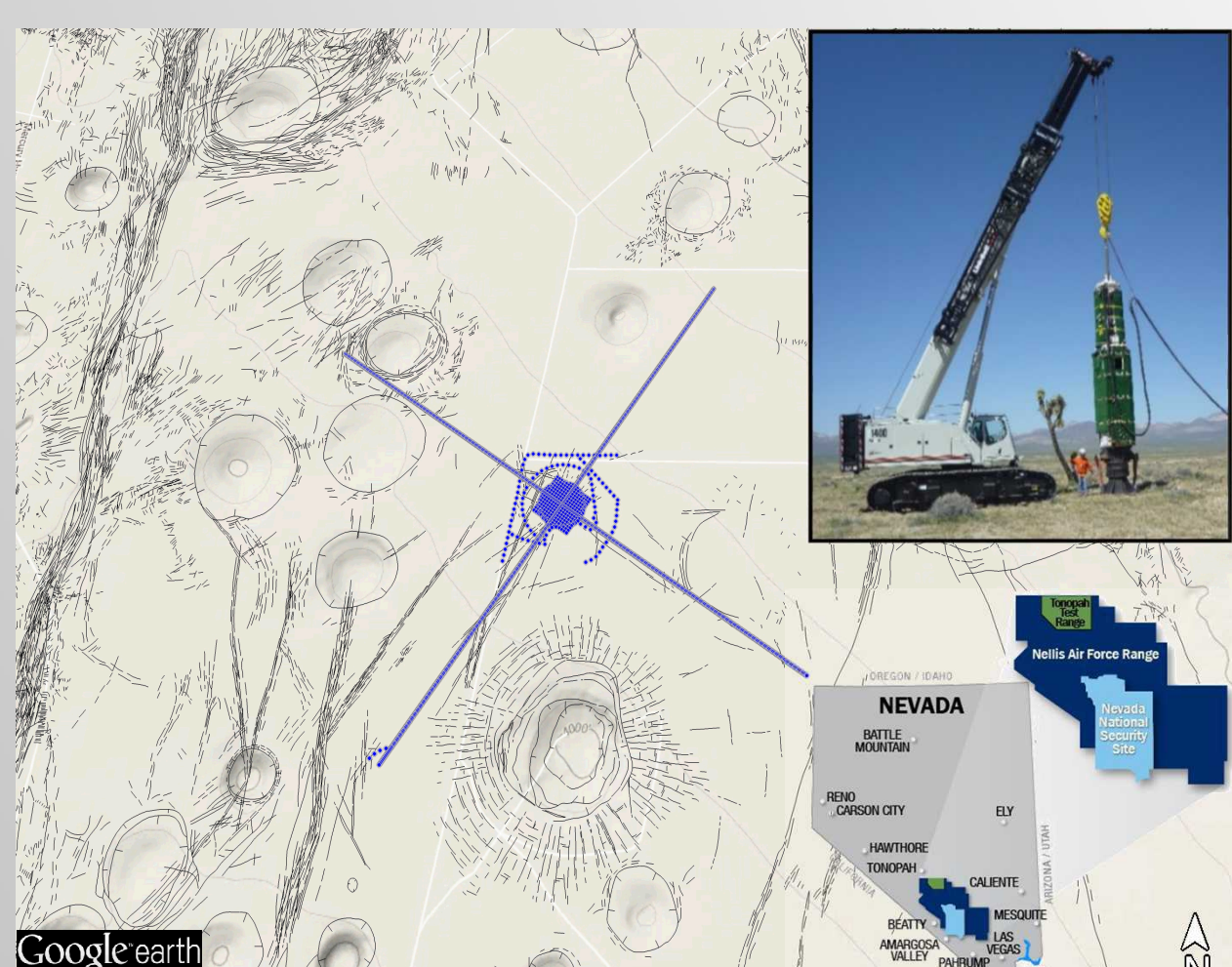


Figure 1: Map of area around HADDOCK (showing visible surface craters from other tests) with shot locations marked in blue. Top right inset shows Seismic Hammer. Lower right inset shows location of Nevada National Security Site.



Figure 2: Predicted scattering locations and intensities. Colorbar gives scattering intensity values. Note the consistently high scattering on the northwest arm in the vicinity of the fault denoted in the cross-section. The crack map is from Grasso, 2001.

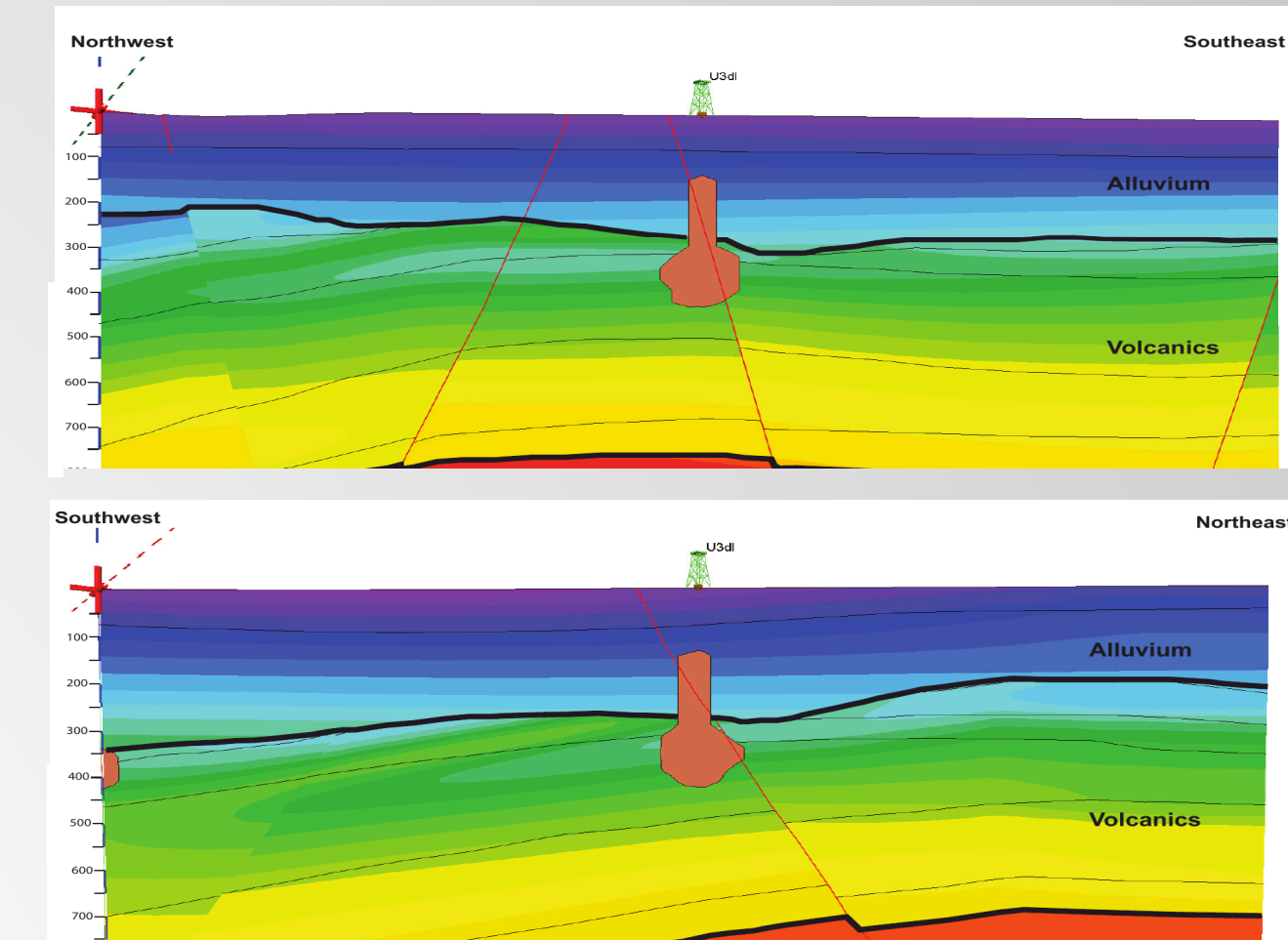


Figure 4: Geologic cross-sections of subsurface surrounding HADDOCK along shot lines. Courtesy of Lance Prothro (NSTec). Faults shown as red lines.

Analysis

To quantify the scattering intensity, the P- and S-wave arrivals were manually picked for each shot. Once the P-coda was isolated for each shot, the Hilbert transform was used to determine the instantaneous amplitude. Each trace was divided into 15 ms sub-intervals, and the average amplitude for each sub-interval and axis was calculated. To calculate scattering intensity, we computed the ratio of rotational energy and translational energy (Figure 3). In this manner, each sub-interval was mapped to a spatial location on an arm of the shot array. All analysis was performed in Python using the ObsPy toolbox.

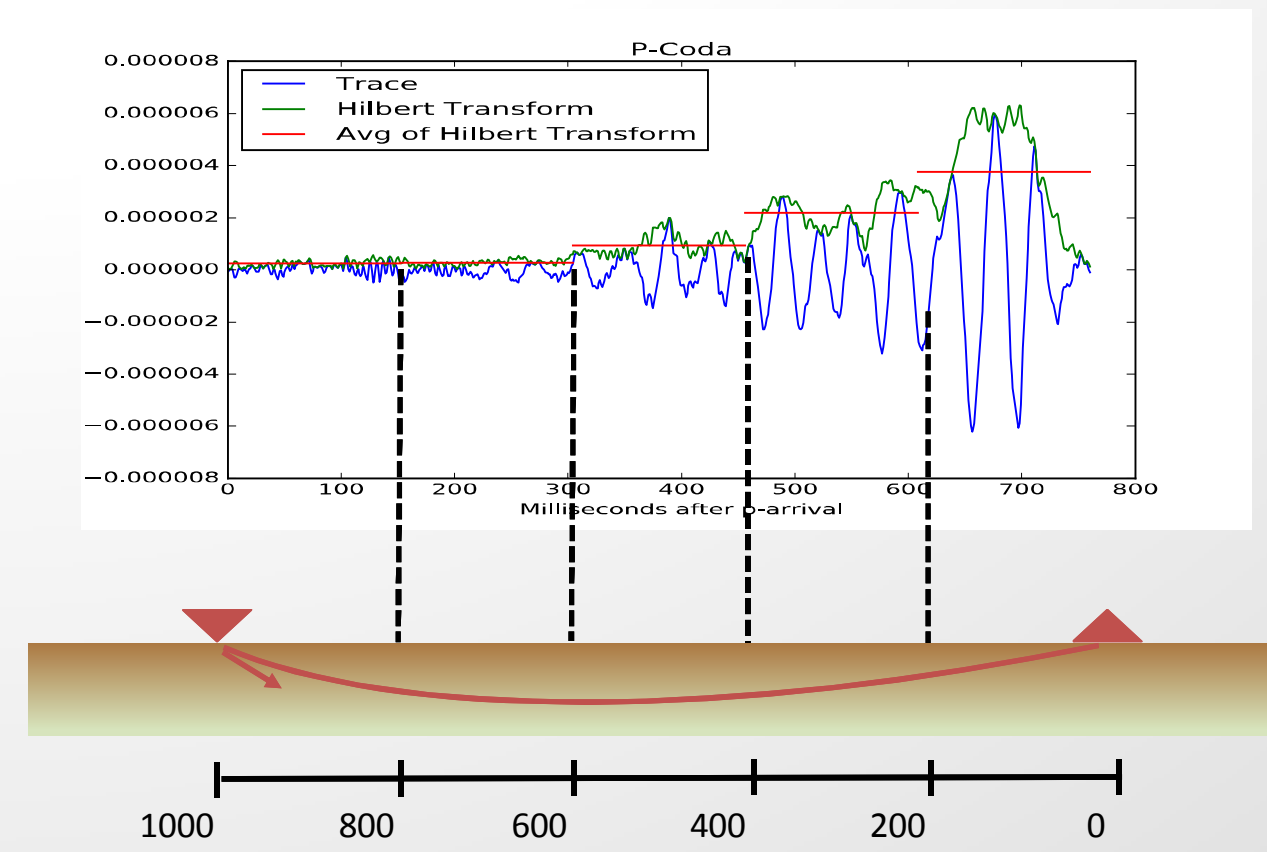


Figure 3: For each axis of motion, the average amplitude value in each subinterval of the P-coda is determined and mapped to a spatial location between the source and receiver. To determine scattering the ratios of rotational and translational values are taken.

Conclusions and Future Work

The results appear consistent with theory for the northwest arm (see Figure 2). There is a region of high scattering that is consistent with a fault location. However, the fault on the southwest arm does not result in the same type of localized high scattering. This may be due to the fault orientation relative to the source-receiver raypath. In order to determine whether this is the case, more work must be done.

- P-wave tomography to get accurate raypaths
- Rotate sensor components perpendicular to the raypath
- Generalize single-scatter theory to multiple scatterers

References

- M. Beyreuther, R. Barsch, L. Krischer, T. Megies, Y. Behr and J. Wassermann (2010), *ObsPy: A Python Toolbox for Seismology*, SRL, 81(3), 530-533 DOI: 10.1785/gssrl.81.3.530
- Grasso, D.N., 2001. *GIS surface effects archive of underground nuclear detonations conducted at Yucca Flat and Pahute Mesa, Nevada Test Site, Nevada* (No. USGS OFR 01-272). United States Geological Survey-Nevada, Las Vegas, NV (US).

Acknowledgements

Special thanks to Hunter Knox of Sandia National Laboratories and Michael Hubenthal of IRIS for his administrative support. We thank Bob White, Frank Spenia, and Jesse Bonner, Ping Lee, and Ray Keegan for their help in acquiring the field data and with NNSS site access and training issues.

Sandia National Laboratories is a multimission laboratory managed and operated by National Technology and Engineering Solutions of Sandia LLC, a wholly owned subsidiary of Honeywell International Inc. for the U.S. Department of Energy's National Nuclear Security Administration under contract DE-NA0003525